Forestry Research

ARTICLE

Open Access

https://doi.org/10.48130/fr-0023-0029

Forestry Research **2024**, 4: e001

Main drivers of vertical and seasonal patterns of leaf photosynthetic characteristics of young planted *Larix Olgensis* trees

Qiang Liu[1], Zhidong Zhang[1], Dongzhi Wang[1], Fengri Li[2*] and Longfei Xie[3]

[1] *School of Forestry, Hebei Agricultural University, Baoding 071000, PR China*
[2] *School of Forestry, Northeast Forestry University, Harbin 150040, PR China*
[3] *School of Forestry, Beihua University, Jilin 132000, PR China*
* Corresponding author, E-mail: fengrili@126.com

Abstract

Photosynthetic characteristics of tall trees play important roles in improving the accuracy of ecosystem models, but they are laborious to be accurately measured or estimated owing to the influence of multiple factors. To clarify the main drivers of vertical and seasonal patterns of leaf photosynthetic characteristics of young planted *Larix Olgensis* trees, we collected data on the photosynthetic, morphological, and meteorological characteristics by a long-term observation throughout the entire growing season. Vertical and seasonal patterns of leaf photosynthetic characteristics and their impact factors were analyzed. Results showed that maximum net CO_2 assimilation (A_{max}), light saturated stomatal conductance ($g_{s\text{-}sat}$), respiration rate (R_D), needle mass per area (NMA), and ratio of needle length to needle width (r_{lw}) all significantly and negatively correlated with relative depth into crown (RDINC), that was caused by the adaptive alteration of mesophyll tissue to the differed light intensity and humidity. A_{max} and $g_{s\text{-}sat}$ both showed a similar 'parabolic' seasonal trend, that was not only affected by the variation of environment but also the leaf economic spectrum, such as NMA. Our results suggested that spatiotemporal variations of crown photosynthetic characteristics were directly influenced by leaf economic spectrum but fundamentally affected by the long-term acclimation to surrounding environmental factors. This is helpful to optimize the crown photosynthesis model to assess instantaneous or even long-term photosynthetic production, in order to clarify the balance of supply and demand within crown, and further guide the effective pruning for individual trees.

Citation: Liu Q, Zhang Z, Wang D, Li F, Xie L. 2024. Main drivers of vertical and seasonal patterns of leaf photosynthetic characteristics of young planted *Larix Olgensis* trees. *Forestry Research* 4: e001 https://doi.org/10.48130/fr-0023-0029

Introduction

Photosynthetic characteristics are indicative of physiological parameters that correlate with forest primary production[1] and drive carbon uptake[2]. They directly participate in the natural carbon cycle but are sensitive to environmental conditions; they are often used to represent the resistance and resilience of vegetation to extreme climates[3], pests and diseases[4,5], fires[6], and toxic metals[7,8]. Convergent emergence or loss of photosynthetic phenotypes may facilitate adaptation to ecologically similar environments[9].

In forestry, differences in photosynthetic characteristics among different tree species are prominent[10]. The photosynthetic characteristics of leaves within the same species often have significant spatial heterogeneity owing to the complex spatial structure of the crown[11], which is particularly evident in the vertical structure of the crown[12,13]. Light[14,15] and water potential[16] are thought to be the key determining factors of vertical variation patterns in tree crown photosynthetic traits. However, the dominant roles of two species could shift under different forest densities and tree sizes. Generally, in closed canopies, light is the major factor that leads to the spatial heterogeneity of leaf photosynthetic traits[17], causing leaves to alter their structure and physiological function to adapt to the lighting environment. Likewise differences appear between shade and sun leaves within the crown[13]. Sun leaves have a high maximum net CO_2 assimilation (A_{max}), respiration rate (R_D), and light compensation point (LCP) but lower light utilization efficiency (LUE) and light saturation point (LSP)[18]. Water potential tends to be the dominant factor for huge dominant trees[19], as it represents the ability to transport the water from the root to the crown. Crown photosynthetic characteristics also show seasonal variation with individual development and environmental changes[20,21]. For example, A_{max} usually shows a parabolic seasonal variation pattern due to its positive correlation with the temperature (T), solar radiation, and soil moisture[22–24]. However, R_D exhibits an opposite 'U'-shaped trend[18] due to the decline of cytochrome-mediated respiration[21] and temperature sensitivity[25].

Studies have shown that spatial and seasonal variations in canopy photosynthetic characteristics are closely associated with the comprehensive impact of light[26], temperature[24,27], humidity[28], and seasonal patterns of leaf structural traits[29,30]. Generally, adequate light and suitable temperature and humidity can promote photosynthesis, by improving light energy utilization[31] and photosynthetic enzyme activity[32], however, some environmental conditions will inhibit photosynthesis[33]. For example, the common natural phenomena 'midday depressions' is a self protection mechanism by regulating blade osmotic pressure and maintaining mesophyll cell activity, in response to the stress of strong light, high temperature and low humidity[34]. Additionally, the age[22,35,36] and sex of dioecious tree species[37] influence the photosynthetic characteristics of leaves to some extent due to the difference of mesophyll cell structure. When simulating the mechanism process

model of canopy, forest productivity, and carbon absorption processes, the spatial and seasonal variations in canopy leaf photosynthetic characteristics need to be considered simultaneously, otherwise, incorrect results will be obtained[16]. Therefore, the spatiotemporal heterogeneity and driving mechanisms of canopy photosynthetic characteristics need to be urgently clarified.

This study used the artificial forest of the main afforestation species (*Larix olgensis*) in the northern area of China as the research object that was tracked and monitored throughout its growing season. The factors of photosynthetic characteristics, leaf morphology, crown structure and environmental factor were collected. The overarching aims of this study are twofold: first, is there a significant difference in photosynthetic characteristics of different crown positions, growing periods and tree individuals? Secondly, what is the variation patterns of photosynthetic characteristics within the tree crown during the growing season? Finally, we provide a comprehensive assessment of the relationships between photosynthetic characteristics and crown structure, leaf morphology and environmental conditions.

Materials and methods

Site description

The experiments were conducted in 2017 at the experimental forest farm of Northeast Forestry University in Maoershan, Haerbin, China (Northern latitude: 45°2′20″~45°18′16″, East longitude: 127°18′0″~127°41′6″; altitude 400 m above sea level). The climate in the Maer Mountain region belongs to the temperate continental monsoon climate, with an average annual temperature of 2.4 °C, the highest temperature being 34 °C and the lowest being −40 °C, approximately 125 d of frost-free period, an average annual precipitation of 700 mm, and dark brown soil as the main type. Total forest coverage is approximately 83.3%, including 14.7% plantation.

Sample selection

Five fixed plots of 20 m × 30 m with same site quality in the young *L. olgensis* plantation are set up, and the trees with a diameter at breast height (DBH) larger than 5 cm in each plot were measured. The specific measurement factors include tree height (H), DBH, crown width (CW) and the relative coordinates (x_i, y_i) of each tree were investigated. Then the average DBH of five plots were calculated according to the per tree measurement data. A scaffold was built around the sample tree, ensuring that the sample tree was completely surrounded by it, ensuring that all branches of the sample wood and each position of each branch can be measured on the scaffold, each layer is connected by a walkway. After each measurement, the upper tread was removed to avoid the influence on the measurement result caused by the blocking of light. The crown length of each sample tree was divided into several vertical sections based on the whorls from tree top to bottom and numbering began from V1st. Three healthy and fully expanded needles located within each section in the middle of the foliated branches in sunny, semisunny and shaded crowns were selected, according to the sample selection principles based on Liu et al.[38]. The photosynthetic characteristics in each vertical section was the average values of measurements taken from different directions (sunny, semisunny and shaded crown).

Photosynthetic gas exchange measurements

The photosynthetic light response (PLR) curves were measured twice per month (the beginning of the month and mid-month) during the growing season (from approximately May 15th to September 10th). All photosynthetic properties were measured with a portable steady-state photosynthesis system (LI-6400XT, LI-COR, Inc., Lincoln, NE, USA) equipped with a standard LED light source (6400-02B, LI-COR, Inc., Lincoln, NE, USA). Sample chamber was acclimated for 20 min at a CO_2 concentration of 390 ppm with a CO_2 mixer (6400-01, LI-COR, Inc., Logan, NE, USA) to maintain a stable CO_2 supply. All sample cluster needles were acclimated under a PAR of 1,400 μmol·m^{-2}·s^{-1} for 10 to 20 min by the LED light source (6400-02B, LI-COR, Inc., Lincoln, NE, USA). PLR curve was measured at 10 PAR gradients: 2,000, 1,500, 1,200, 1,000, 500, 200, 150, 100, 50, 0 μmol·m^{-2}·s^{-1}. Sample cluster needles were allowed to equilibrate for a minimum of 2 min at each measurement before data was logged, and a calibration (match) was performed after each count. At the same time, the temperature of the leaf (Air temperature, Tair), the relative humidity (Relative humidity, RH) and the vapor pressure deficit (Vapor pressure deficit, VPD) were recorded. After the measurements, the depth into the crown (Depth into crown, DINC) of each measured sample was recorded in the crown, and the relative depth into the crown (Relative depth into crown, RDINC) was calculated according to the crown length (Crown length, CL): RDINC = DINC/CL.

Needle morphology measurements

Once the photosynthetic gas exchange measurements were completed, the sample cluster needles were immediately taken back to the laboratory for measuring the needle mass per area (NMA, g·m^{-2}). Each cluster sample was scanned immediately after collection and then surveyed with an image analysis software (Image-Pro Plus 6.0, Media Cybernetics, Inc., Bethesda, USA), resulting in the projected needle area (NA, m^2), needle length (l) and needle width (w), and consequently obtained the ratio of needle length to needle width (r_{lw}). Then, the scanned samples were dried to a constant weight at 85 °C and weighed to dry weight (WD). The NMA was calculated: NMA = WD/LA.

Photosynthetic parameters

The light-saturated CO_2 assimilation (A_{max}, μmol·m^{-2}·s^{-1}) and dark respiration (R_D, μmol·m^{-2}·s^{-1}) were estimated from the PLR curves using the modified Mitscherlich model[39]:

$$A_n = A_{max} \times \left(1 - e^{(-\alpha \times PAR/A_{max})}\right) - R_D \quad (1)$$

where A_n is the net CO_2 assimilation (μmol·m^{-2}·s^{-1}), A_{max} is the light-saturated net CO_2 assimilation (μmol·m^{-2}·s^{-1}), α is the apparent quantum yield, PAR is the photosynthetically active radiation (μmol·m^{-2}·s^{-1}), and R_D is the dark respiration rate (μmol·m^{-2}·s^{-1}).

The light saturated stomatal conductance ($g_{s\text{-}sat}$, mol·m^{-2}·s^{-1}) was determined as the corresponding gs value of A_{max}. Water-use efficiency (WUE_{sat}, mmol CO_2 mol H_2O^{-1}) was calculated as the ratio of A_{max} to $g_{s\text{-}sat}$. As the environment conditions were not maintained under a certain value during the measurement of PLR curves except CO_2 concentration (stabilized at 390 ppm).

Statistical analysis

Table 1 shows the data summary. Statistical analyses were performed using R software 4.2.2[40]. A three-way repeated-measures analysis of variance (ANOVA) was performed on all

Table 1. Sample tree and data summary. Photosynthetic light response curves (752) were investigated, including 9303 instantaneous environmental and functional factors, from 36 pseudowhorls from five planted *Larix olgensis* trees.

Statistics	Net photosynthetic rate	Leaf trait	Environmental conditions			Spatial position
	A_n (μmol·m^{-2}·s^{-1})	LMA (g·m^{-2})	T_{air} (°C)	VPD (kPa)	PAR (μmol·m^{-2}·s^{-1})	RDINC
No.			9303			752
Mean	5.23	58.5	27.9	1.7	757	0.52
Std.	4.47	20.1	3.6	7	723	0.26
Max.	27.49	127.5	39.4	4.3	2200	0.99
Min.	−3.90	14.3	15.5	0.5	0	0.08

A_n, net CO_2 assimilation; LMA, leaf mass per area; T_{air}, air temperature; VPD, vapor pressure deficit; PAR, photosynthetically active radiation; RDINC, relative depth into the crown (RDINC). No., Mean, Std., Max. and Min. are the numbers, mean value, standard deviation, maximum value and minimum value, respectively.

experimental variables to evaluate the effects of individual tree (T), period (P), and crown layer (L) on light-saturated CO_2 assimilation (A_{max}), dark respiration (R_D), light-saturated stomatal conductance ($g_{s\text{-}sat}$), and water-use efficiency (WUE_{sat}). Pearson's correlation analysis was used to test the relationships among all the measured variables. The significance of all the statistical analyses was at $\alpha = 0.05$ level. All figures were drawn using the ggplot2 package in R software 4.2.2.

Results

Vertical profiles of photosynthetic and morphological parameters of needles

Photosynthetic parameters (A_{max}, R_D, $g_{s\text{-}sat}$ and WUE_{sat}) and morphological parameters (LMA and r_{lw}) differed significantly among the different measurement phases, individual trees, and vertical locations of the crown (Table 2). Considering the average pattern across the five sample trees, nearly all physiological and morphological parameters of the needles exhibited a similar vertical profile, which decreased noticeably with increasing RDINC (Fig. 1). However, the mean WUE_{sat} of the five sampled trees followed the opposite trend (Fig. 1f). A_{max} significantly decreased with RDINC (Fig. 1a), and the mean A_{max} in the top crown (12.84 μmol·m^{-2}·s^{-1}) was almost 2.7 times higher

Table 2. Results of the three-way repeated measures ANOVA of photosynthetic and morphological parameters.

Effects	df	A_{max}	$g_{s\text{-}sat}$	R_D	WUE_{sat}	NMA	r_{lw}
T	***	***	***	***	***	***	*
P	***	***	***	***	***	***	***
L	***	***	***	***	***	***	***
T×P	***	***	***	***	***	*	***
T×L	*	***	***	***	***	***	
P×L	***	***	***	***	***	***	*
T×P×L	***	**	***		***		

P, measurement period; T, tree specific; L, crown location. The different parameters have been identified and described in the text. *, $0.01 < p \leq 0.05$; **, $0.001 < p \leq 0.01$; ***, $p \leq 0.001$.

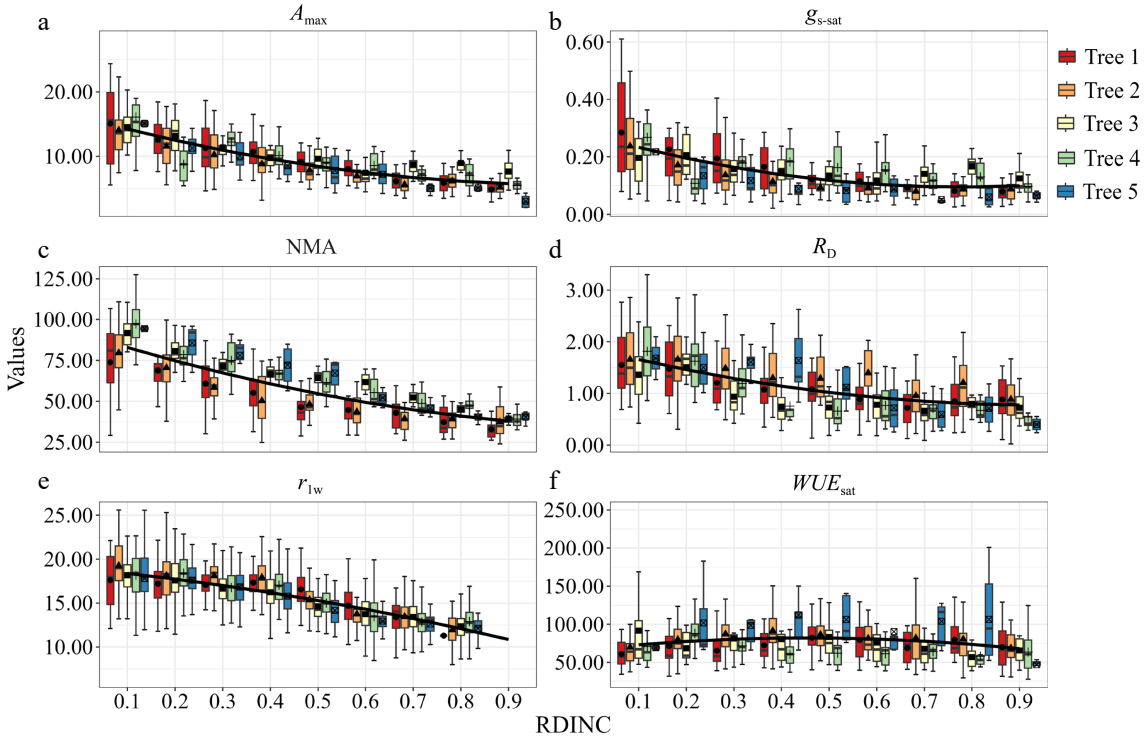

Fig. 1 Vertical profiles of (a) light-saturated net photosynthetic rate (A_{max}); (b) light-saturated stomatal conductance ($g_{s\text{-}sat}$); (c) needle mass per area (NMA); (d) dark respiration (R_D); (e) ratio of length to width of needles (r_{lw}) and (f) light-saturated water use efficiency (WUE_{sat}). Data points represented seasonal mean values (solid bars represented stand error). Black solid line represented mean values of five sample trees (a)–(f).

than that in the bottom crown (4.81 μmol·m^{-2}·s^{-1}). Although there were significant tree-specific differences in $g_{s\text{-}sat}$, NMA, and R_D (Table 2), their tendencies demonstrated a pronounced decrease with increasing RDIINC (Fig. 1b, c, & d). The mean values of R_D, $g_{s\text{-}sat}$, and NMA varied by 2.5-fold, 3.3-fold, and 2.3-fold, respectively, from the top to the bottom of the crown. Mean r_{lw} exhibited a slight decrease with RDINC when RDINC was lower than 0.3 (upper crown) (Fig. 1e) but then sharply decreased when RDINC was greater than 0.4 (middle and lower crown). In contrast, mean WUE_{sat} showed a weak upward trend with increasing RDINC (Fig. 1f), varying by only 0.015 mmol CO_2 mol H_2O^{-1} from top to bottom.

As mentioned above, photosynthetic and morphological parameters were significantly affected by the vertical location of the crown. However, it is unknown whether the same pattern remains during the entire growth period. Analysis of variance was performed on photosynthetic and morphological parameters based on the vertical locations (upper, middle, and lower crown) in each measurement phase, and the results are summarized in Table 3. r_{lw} was the only parameter that showed a significant vertical difference across the entire growth season (upper > middle > lower crown). A_{max}, $g_{s\text{-}sat}$, and NMA demonstrated a similar vertical pattern in June, but the mean values of A_{max} and $g_{s\text{-}sat}$ were not significantly different between the upper and middle crown during the early period of needle expansion (PI, May). Mean NMA showed no significant vertical difference within the crown. R_D showed no significant difference with respect to vertical location in the crown during the early period of needle expansion but showed significantly greater values in the upper crown than in the middle and lower crowns after June. WUE_{sat} only showed a slight vertical difference at PVI, PVII, and PIV.

Seasonal variation of photosynthetic and morphological parameters of needles

All photosynthetic and morphological parameters differed significantly among the individual sample trees and fluctuated during the growing seasons (Fig. 2). Mean daily A_{max} increased with time until late summer (at early August) to a maximum of nearly 9.42 μmol·m^{-2}·s^{-1} (Fig. 2a). For the remaining season, mean A_{max} ranged from 8.25 μmol·m^{-2}·s^{-1} to 8.34 μmol·m^{-2}·s^{-1}. The mean daily R_D exhibited a significant decrease over time in early summer to a minimum of near 0.77 μmol·m^{-2}·s^{-1} and was then restored to 1.04 μmol·m^{-2}·s^{-1} (Fig. 2d). $g_{s\text{-}sat}$ and NMA exhibited a similar time course with an increase during the growing season (Fig. 2b and 2c), but an abnormal peak appeared in early August. Mean WUE_{sat} demonstrated a time course that is opposite to that of $g_{s\text{-}sat}$ and NMA (Fig. 2f). Mean NMA increased abruptly at the early period of needle expansion (PI, May), then remained stable until the second half of August (PVII), but finally increased at the end of growth.

Correlations between photosynthetic and meteorological parameters

The relationships between photosynthetic and main meteorological parameters are shown in Fig. 3. A_{max} significantly correlated to T_{leaf}, RH, and VPD in the entire treatment (Fig. 3a–c), in which A_{max} positively correlated to T_{leaf} and RH but negatively correlated to VPD. The correlation was stronger between A_{max} and RH (r = 0.46) than between A_{max} versus T_{leaf} (r = 0.27) and VPD (−0.28). R_D positively and linearly correlated with VPD (r = 0.31, Fig. 3i), but a stronger nonlinear relationship was observed between R_D and T_{leaf} (r = 0.61, Fig. 3g). RH poorly correlated with R_D (r = 0.07, Fig. 3h). $g_{s\text{-}sat}$ significantly and nonlinearly correlated with RH (positive) and VPD (negative) (Fig. 3e & f). In contrast, WUE_{sat} negatively correlated with RH (r = −0.65, Fig. 3k), positively correlated with VPD (r = 0.64, Fig. 3l), and weakly correlated with T_{leaf} (r = 0.3, Fig. 3j).

Relationships between physiological parameters and LMA

A_{max} and R_D exhibited a positive and significant correlation with LMA (Fig. 4a & c), but there were slight differences in the correlation coefficients among the individual sample trees. Although $g_{s\text{-}sat}$ showed a similar correlation with LMA as A_{max} and R_D, the correlation was weaker (r = 0.35, Fig. 4b). WUE_{sat} only significantly correlated with LMA for two sample trees,

Table 3. Summary of physiological and morphological parameters in upper, middle, and lower crown, respectively during growing seasons.

Factors	Location	PI	PII	PIII	PIV	PV	PVI	PVII	PVIII
A_{max} (μmol·m^{-2}·s^{-1})	Upper	7.07 ± 0.18^a	8.67 ± 0.51^a	9.77 ± 0.89^a	12.11 ± 1.48^a	12.16 ± 0.74^a	14.18 ± 1.33^a	13.74 ± 1.42^a	11.42 ± 0.85^a
	Middle	6.76 ± 0.23^a	7.19 ± 0.66^b	7.82 ± 0.75^b	9.19 ± 0.82^b	9.03 ± 0.54^b	9.03 ± 1.24^b	8.11 ± 0.77^b	7.88 ± 0.38^b
	Lower	5.80 ± 0.12^b	5.93 ± 1.1^c	6.57 ± 0.78^c	6.03 ± 0.97^c	6.48 ± 1.07^c	5.15 ± 1.19^c	4.3 ± 1.71^c	5.47 ± 0.86^c
R_D (μmol·m^{-2}·s^{-1})	Upper	1.51 ± 0.12^a	1.35 ± 0.23^a	1.25 ± 0.12^a	1.13 ± 0.28^a	1.35 ± 0.25^a	1.36 ± 0.19^a	1.30 ± 0.15^a	1.46 ± 0.10^a
	Middle	1.37 ± 0.11^a	1.01 ± 0.25^b	0.96 ± 0.17^b	0.80 ± 0.18^b	0.66 ± 0.11^b	0.99 ± 0.23^b	0.90 ± 0.14^b	1.11 ± 0.14^b
	Lower	1.46 ± 0.03^a	0.74 ± 0.27^c	0.83 ± 0.20^b	0.65 ± 0.13^b	0.51 ± 0.10^b	0.96 ± 0.44^b	0.71 ± 0.20^c	1.04 ± 0.18^b
$g_{s\text{-}sat}$ (mol·m^{-2}·s^{-1})	Upper	0.090 ± 0.01^a	0.117 ± 0.03^a	0.118 ± 0.01^a	0.164 ± 0.02^a	0.168 ± 0.02^a	0.297 ± 0.06^a	0.241 ± 0.05^a	0.223 ± 0.02^a
	Middle	0.074 ± 0.01^a	0.082 ± 0.02^b	0.089 ± 0.01^b	0.109 ± 0.01^b	0.114 ± 0.01^b	0.174 ± 0.04^b	0.125 ± 0.02^b	0.132 ± 0.02^b
	Lower	0.047 ± 0.01^b	0.058 ± 0.02^c	0.075 ± 0.02^c	0.078 ± 0.01^c	0.083 ± 0.02^c	0.117 ± 0.03^c	0.063 ± 0.02^c	0.085 ± 0.03^c
WUE_{sat} (mmol·mol^{-1})	Upper	92.1 ± 9.6^a	93.3 ± 22.1^a	102.1 ± 11.4^a	79.7 ± 8.0^{ab}	76.0 ± 9.5^a	58.9 ± 8.1^b	61.1 ± 6.6^b	62.5 ± 3.8^a
	Middle	92.0 ± 7.2^a	91.0 ± 22.5^a	94.0 ± 7.0^a	84.2 ± 6.0^a	88.0 ± 9.3^a	69.5 ± 8.4^a	71.7 ± 12.3^a	63.9 ± 5.0^a
	Lower	113.7 ± 7.9^a	78.8 ± 14.3^a	93.6 ± 15.9^a	76 ± 12.8^b	88.4 ± 25.6^a	58.1 ± 16.4^b	57.1 ± 16.6^b	63.1 ± 13.4^a
NMA (g·m^{-2})	Upper	37.8 ± 1.5^a	58.6 ± 4.7^a	69.6 ± 5.0^a	74.5 ± 5.7^a	77.9 ± 6.0^a	91.7 ± 6.1^a	83.9 ± 6.1^a	74.6 ± 6.5^a
	Middle	36.4 ± 2.2^a	51.2 ± 4.5^b	53.9 ± 4.6^b	59.4 ± 5.6^b	56.7 ± 5.1^b	66.9 ± 5.3^b	60.8 ± 5.4^b	56.2 ± 5.4^b
	Lower	29.1 ± 1.1^a	35.9 ± 5.0^c	40.4 ± 5.7^c	42.9 ± 5.6^c	39.6 ± 5.6^c	45.6 ± 5.5^c	44.1 ± 5.5^c	40.8 ± 5.5^c
r_{lw}	Upper	14.2 ± 0.06^a	17.8 ± 0.10^a	18.6 ± 0.10^a	18.0 ± 0.08^a	17.7 ± 0.10^a	17.9 ± 0.11^a	17.4 ± 0.11^a	18.6 ± 0.12^a
	Middle	12.9 ± 0.07^b	15.7 ± 0.08^b	15.3 ± 0.08^b	15.2 ± 0.09^b	14.9 ± 0.08^b	14.4 ± 0.11^b	14.9 ± 0.09^b	16.2 ± 0.10^b
	Lower	11.5 ± 0.08^c	13.3 ± 0.11^c	13.3 ± 0.09^c	13.0 ± 0.10^c	13.5 ± 0.14^c	12.6 ± 0.10^c	12.9 ± 0.11^c	13.6 ± 0.11^c

Values are Mean ± SE. Mean values with same superscript do not differ significantly ($p < 0.05$).

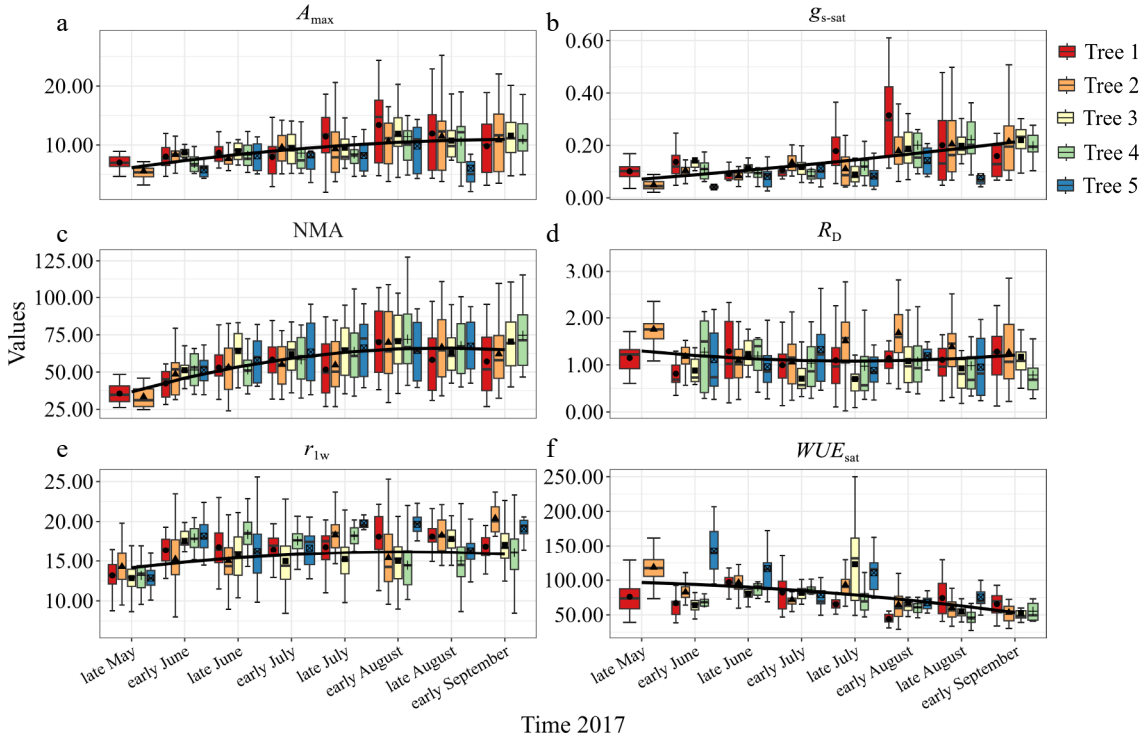

Fig. 2 Seasonal evolution of (a) light-saturated net photosynthetic rate (A_{max}); (b) light-saturated stomatal conductance ($g_{s\text{-}sat}$); (c) needle mass per area (NMA); (d) dark respiration (R_D); (e) ratio of length to width of needles (r_{lw}) and (f) light-saturated water use efficiency (WUE_{sat}) for five sample trees. Data points represent seasonal mean values (solid bars represented stand error). Black solid line represented corrective mean values of five sample trees (a)–(f).

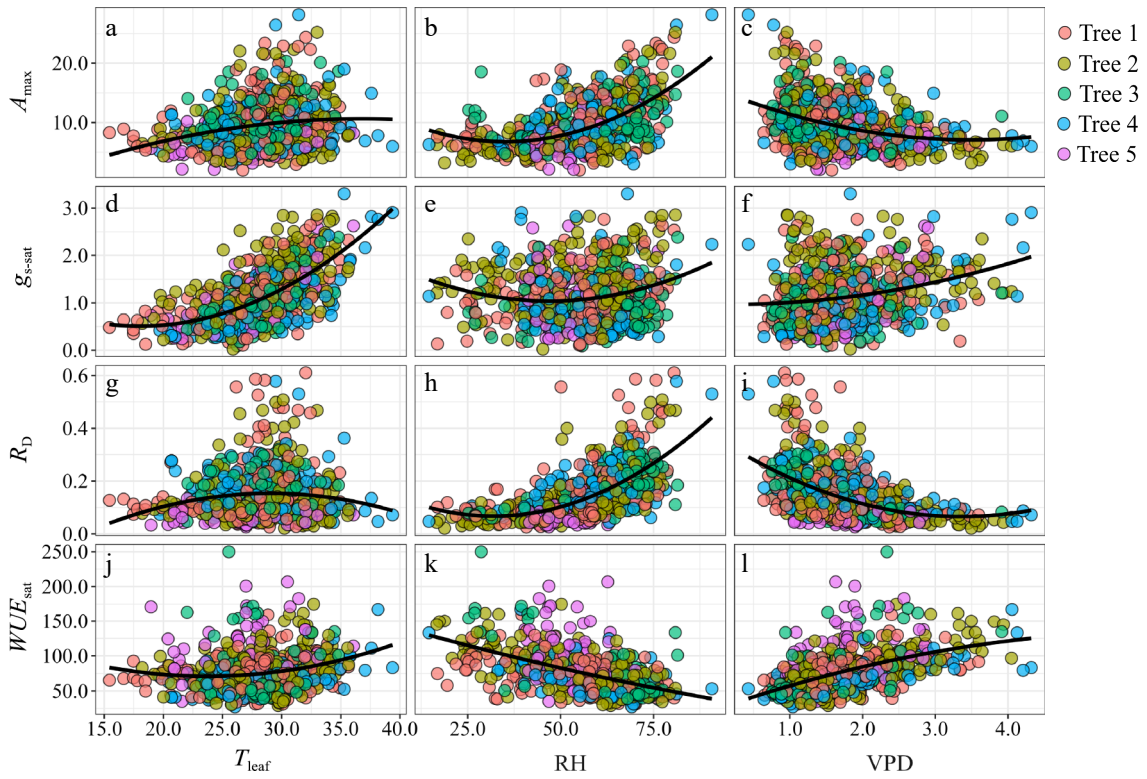

Fig. 3 Relationship between light-saturated net photosynthetic rate (A_{max}), light saturated stomatal conductance ($g_{s\text{-}sat}$), dark respiration (R_D), and light-saturated water use efficiency (WUE_{sat}) and (a), (d), (g), (j) leaf temperature (T_{leaf}); (b), (e), (h), (k) relative humidity (RH); and (c), (f), (i), (l) vapor pressure deficit (VPD) for five trees.

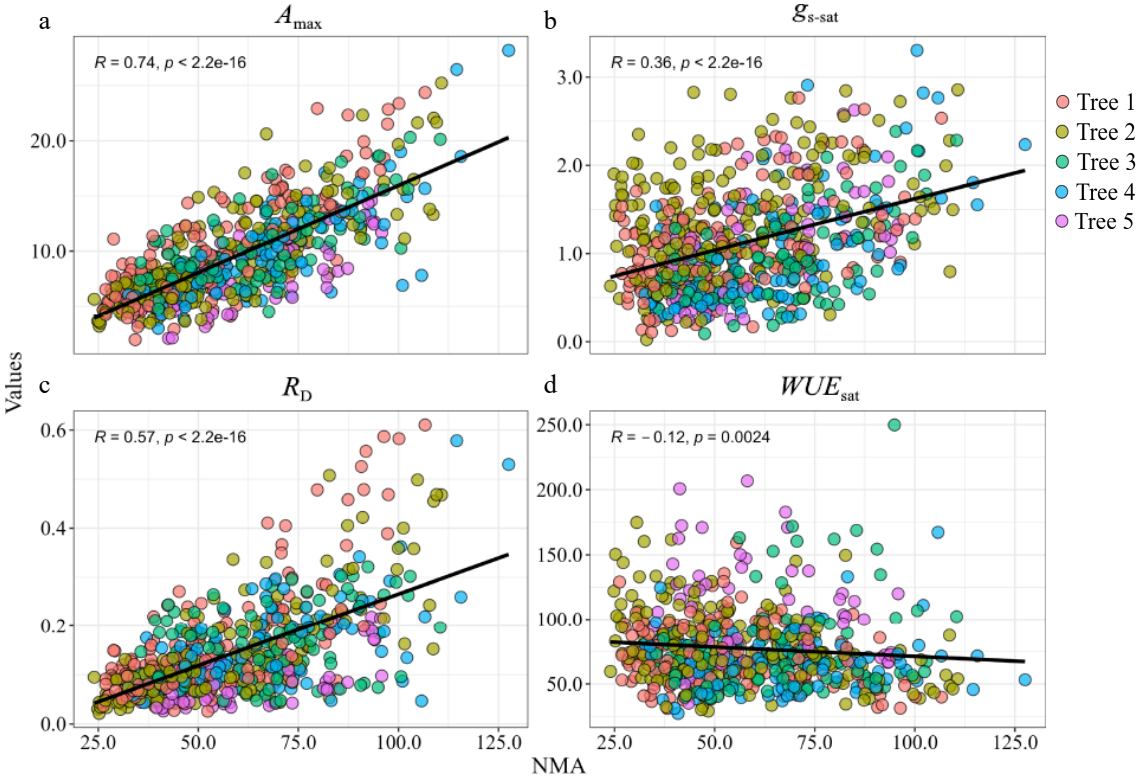

Fig. 4 Relationships between (a) light-saturated net photosynthetic rate (A_{max}) and needle mass per area (NMA); (b) light-saturated stomatal conductance ($g_{s\text{-}sat}$) and NMA; (c) dark respiration (R_D) and NMA; (d) light-saturated water use efficiency (WUE_{sat}) and NMA. R values are the Pearson correlation coefficients. Solid lines represent the fitting result and are based on linear equations.

even although a significantly negative relationship was observed for all the sample trees (Fig. 4d). WUE_{sat} negatively correlated with LMA but was more significant seasonally than spatially.

Discussion

Spatial variation of needle physiology and morphology

Previous studies have suggested that light[15] and water potential[19,41] are the most important factors affecting the vertical pattern of leaf physiology and morphology, but the primary driver between these two factors is still being debated[42]. Recently, it has become increasingly accepted that the effects of these two factors vary with tree height[43]. Light reportedly affects leaf functions and structures in short trees[15,19], but for tall trees, a decrease in water potential considerably limits their leaf expansion and photosynthetic rate[44]. Our results showed that A_{max} and $g_{s\text{-}sat}$ decreased significantly from crown top to bottom (Fig. 1a & c), which is consistent with that of other studies[45]. Martin et al. reported that shade leaves growing under less irradiance had lower leaf stomatal conductance than sun leaves[18]. R_D negatively correlated with RDINC (Fig. 1b), as previously documented for different species[46], because leaves generally adapted to dark environments by reducing R_D and Non-photochemical quenching. High leaf tissue density[15] decreased mesophyll conductivity to gas, and restrained R_D[45], which was also proved by the higher positive correlation between R_D and NMA (Fig. 4c). The vertical pattern of R_D partly decreased A_{max} with increasing tree height but was not significant. NMA is one of the main morphological traits that changes in response to light variations[47]; thus, in our study, NMA followed the same pattern as A_{max}, $g_{s\text{-}sat}$, and R_D (Fig. 1e), suggesting that needles synthesize more photosynthetic tissue with increasing height to maximally use sufficient illumination. Studies revealed that the universal NMA gradient within the tree crowns or forest canopies is likely driven by solute content, leaf thickness[48], leaf turgor pressure[45], and leaf tissue density[15], which reflect the plasticity and adaptability of foliage to the environment. Physiological variations in needles are usually accompanied by a corresponding change in their external form[19]. Our results showed that r_{lw} significantly decreased with increasing RDINC (Fig. 1f), which further implied that trees maximized their photosynthetic efficiency by adjusting their foliage morphology to adapt to different environments in the vertical direction. Variations in WUE_{sat} originate from variations in photosynthetic rate, stomatal conductance, or both[49]. Studies showed that WUE_{sat} negatively correlated with $g_{s\text{-}sat}$[50]. In this study, WUE_{sat} showed an opposite vertical tendency to $g_{s\text{-}sat}$ (Fig. 1d), which increased slightly and positively with RDINC, further supporting the opinion that foliage in the lower crown or canopy usually compensates for low resources by improving the utilization efficiency of site resources[51].

Seasonal variation of needle physiology and morphology

Understanding the effect of seasonal variations on physiological and morphological parameters is critical for accurate

modeling of carbon dioxide uptake by ecosystems, which can then be used to determine the magnitude of ecosystem carbon fluxes[52]. Neglect of this variation may result in incorrect simulations of carbon uptake[53]. Previous studies revealed that A_{max} and $g_{s\text{-}sat}$ generally show a trend similar to a typical parabolic curve during the growing season[22,54] although contrary results have been reported[55]. However, A_{max} strongly correlated with $g_{s\text{-}sat}$ in the above investigations, indicating that stomatal behavior has a pronounced impact on A_{max}. Our results show that all the physiological and morphological parameters fluctuated during the growth season. A_{max} had a parabolic seasonal variation, similar to that reported in other studies[22] though accompanied by slight fluctuations in different trees (Fig. 2a), which was probably caused by the high correlation between A_{max} and seasonal variation of environment conditions (Fig. 3)[38]. Kunert et al. confirmed that short-term exposure to high temperatures poses a considerable threat to conifer species in Central European forest production systems[56]. During spring, an increase in A_{max} resulted from a gradual increase in photosynthetic capacity[37]. A decrease in A_{max} during needle senescence is associated with a decrease in mesophyll conductivity to carbon dioxide owing to the increasing size of chloroplasts, starch grains, plastoglobuli, and the resorption of nitrogen[57]. Seasonal variations in leaf photosynthetic traits, including maximum photosynthesis rate, maximum carboxylation rate, and mesophyll and stomatal conductance, can be well explained based on photoperiod variations[2]. In addition, under both winter and drought stress, the main challenge for plants is that electron acceptor regeneration processes markedly slow down compared to primary photosynthetic processes, and this creates an imbalance between absorption and utilization of light energy[28].

Previous studies have suggested that seasonal variations in R_D are mainly driven by seasonal patterns in temperature and NMA[58]. It is well known that starch and soluble sugars are the main reactants in the respiratory process; thus, their content directly affects respiration. Temperature also indirectly limits respiration by affecting the activity of enzymes that participate in respiration[59]. A previous study showed that a reduction in leaf expansion phase was due to a decrease in cytochrome-mediated respiration[21]. Our results implied that R_D was significantly correlated with T_{leaf} (Fig. 3b) and NMA (Fig. 4b). The seasonal pattern of R_D showed an obvious reduction in the leaf expansion phase and then slightly recovered with a little fluctuation (Fig. 2b), following a similar trend in other studies[60].

Table 4. Results of the One-way ANOVA of photosynthetic parameters in each vertical layer.

Vertical layer	Photosynthetic parameters			
	A_{max}	R_D	WUE_{sat}	$g_{s\text{-}sat}$
1	**		**	**
2	**		**	**
3	**		**	**
4	**		**	**
5		*		
6		*		
7		*		
8		*		
9		*		

The different parameters have been identified and described in the text. *, $0.01 < p \leq 0.05$; **, $0.001 < p \leq 0.01$.

NMA showed a progressive increase throughout the growing season (Fig. 2e) owing to the accumulation of structural proteins and calcium. Seasonal variation in WUE_{sat} was different from that in $g_{s\text{-}sat}$ (Fig. 2d), probably because WUE_{sat} and $g_{s\text{-}sat}$ are negatively correlated[49]. Previous studies on seasonal patterns of leaf length, width, and thickness have shown that they universally follow a saturation or parabolic curve[58] throughout the growth season, reflecting the dynamic nature of photosynthetic acclimation[61]. We also observed variations in leaf shape and found that the ratio of length to width (r_{lw}) showed a saturated tendency (Fig. 2f). The increase at the end of the growing season indicated that the needles started to senescence.

A further analysis of seasonal difference in photosynthetic rates among different canopy positions was conducted (Table 4), and the result indicated that A_{max}, WUE_{sat} and $g_{s\text{-}sat}$ were significantly different in the upper crown but not significant in the lower crown. Conversely, R_D showed significant seasonal difference in the lower crown but not significant in the upper crown. Rare studys mentioned relevant results, but some research have proved that photosynthesis was more sensitive to light intensity and respiration was mainly affected by temperature[49–51]. In our study, the closed-canopy caused an obvious seasonal change of light intensity in upper crown, but weak in lower crown. However, the seasonal variation of temperature was evident in the whole crown. Thus, A_{max}, WUE_{sat} and $g_{s\text{-}sat}$ showed different seasonal difference compared to R_D.

Relationship between needle physiology and environment

T_{leaf} showed a significant parabolic correlation with A_{max} (Fig. 3a), corroborating the results of many other studies that focused on different tree species such as, *Quercus crispul*[57], *Picea mariana*[62], *Pinus cembra*[63]. Both RH and VPD showed a significant relationship with A_{max} (Fig. 3e & i), particularly in the upper crown, presumably because needles in the upper crown are exposed to environmental stresses more frequently, and the variations in RH and VPD in the upper crown are more sensitive and greater[64] than that in other crowns. R_D exhibited a typical exponential relationship with T_{leaf} (Fig. 3b), corroborating the results of other studies[46,58,62]. Both $g_{s\text{-}sat}$ and WUE_{sat} significantly correlated with RH (Fig. 3g & h) and VPD (Fig. 3k & l), but the tendencies were diametrically opposite. Similar processes have been observed in other studies[37,50]. Some studies have suggested that variations in WUE_{sat} across dates are primarily driven by $g_{s\text{-}sat}$[49] and our investigation showed that WUE_{sat} significantly correlated to $g_{s\text{-}sat}$ ($r = -0.71$). Thus, we suggest that the relationship among WUE_{sat}, versus RH and VPD is likely caused by the influence of RH and VPD on $g_{s\text{-}sat}$.

Relationship between needle physiology and NMA

NMA plays an important role in predicting foliar physiological function, serves as a parameter in ecosystem modeling, and is used as an indicator for potential growth rate[65]. Our results showed that A_{max} and $g_{s\text{-}sat}$ both had a significant positive correlation with NMA (Fig. 4a & c), similar to the results of previous studies on other species[66]. Other studies have shown a negative relationship between mass-based A_{max} and $g_{s\text{-}sat}$ versus NMA, probably because of the vertical pattern of NMA[44]. Han found a negative relationship between A_{max} and $g_{s\text{-}sat}$ versus NMA for *Pinus densiflora*, probably because of a

higher NMA value (> 200 g·m^{-2}) than that in our study (< 130 g·m^{-2})[67]. Moreover, a NMA value of up to 500 g·m^{-2} for *Pinus monticola* [68], 800 g·m^{-2} for *Sequoia sempervirens* [19], and 1,000 g·m^{-2} for *Pseudotsuga menziesii* and *Pinus ponderosa*[68]; almost all these species are categorized as tall tree species with a negative relationship between A_{max} and NMA. Therefore, we speculate that the relatively low NMA in our study may not be sufficient to limit mesophyll conductivity to carbon dioxide, and consequently, A_{max} and R_D is significantly and positively correlated with NMA, probably because of starch and soluble sugar contents[58]. However, WUE_{sat} had a stronger correlation with RH and VPD than with NMA (Figs 3h, l & 4d), indicating that variations in WUE_{sat} across the growing season were primarily driven by the environment rather than by the needle morphology in this study.

Conclusions

Our study found that the spatial and seasonal variations of crown photosynthetic parameters for *Larix olgensis* were directly influenced by NMA, RH and VPD, in which NMA generally reflected the adaptability of leaves to the environmental factors. Thus, clarifying the response relationships between micro-environment and thinning intensity will contribute to the determination of optimal stand density. In addition, our results make it feasible to estimate the crown photosynthetic production and is helpful to further determine the contribution of branches to the trunk, which is the basis when making a pruning plan to produce no-knots wood and enhance the carbon sink capacity of young forests.

Author contributions

The authors confirm contribution to the paper as follows: study conception and design: Liu Q, Li F, Xie L; data collection: Liu Q, Xie L; analysis and interpretation of results: Liu Q, Zhang Z, Xie L; draft manuscript preparation: Liu Q, Wang D, Zhang Z, Xie L. All authors reviewed the results and approved the final version of the manuscript.

Data availability

The datasets generated during and/or analyzed during the current study are available from the corresponding author on reasonable request.

Acknowledgments

This research was financially supported by the Joint Funds for Regional Innovation and Development of the National Natural Science Foundation of China (Project# U21A20244), National Natural Science Foundation of the People's Republic of China (Project# 32201556), and Talent Introduction Research Project of Hebei Agricultural University (Project# YJ201942). We are deeply indebted to the academic staff, past and present postgraduate students of the Department of Forest Management, School of Forestry, Northeast Forestry University, who collected the data in the field.

Conflict of interest

The authors declare that they have no conflict of interest.

Dates

Received 5 September 2023; Accepted 22 November 2023; Published online 9 January 2024

References

1. Hu Y, Xiang W, Karina VR, Lei P, Deng X, et al. 2022. Photosynthetic and hydraulic traits influence forest resistance and resilience to drought stress across different biomes. *Science of The Total Environment* 828:154517
2. Kinoshita T, Kume A, Hanba YT. 2021. Seasonal variations in photosynthetic functions of the urban landscape tree species *Gingko biloba*: photoperiod is a key trait. *Trees* 35:273–85
3. Fu YH, Li X, Chen S, Wu Z, Su J, et al. 2022. Soil moisture regulates warming responses of autumn photosynthetic transition dates in subtropical forests. *Global Change Biology* 28:4935–46
4. Zhang B, Zhou L, Zhou X, Bai Y, Zhan M, et al. 2022. Differential responses of leaf photosynthesis to insect and pathogen outbreaks: a global synthesis. *Science of The Total Environment* 832:155052
5. Kännaste A, Jürisoo L, Runno-Paurson E, Kask K, Talts E, et al. 2023. Impacts of Dutch elm disease-causing fungi on foliage photosynthetic characteristics and volatiles in *Ulmus* species with different pathogen resistance. *Tree Physiology* 43:57–74
6. Bryant KN, Stenzel J, Mathias J, Kwon H, Kolden CA, et al. 2022. Boosts in leaf-level photosynthetic capacity aid *Pinus ponderosa* recovery from wildfire. *Environmental Research Letters* 17:114034
7. Melki F, Talbi ZO, Jeder S, Louati F, Nouairi I, et al. 2022. Cadmium and lead excess differently affect growth, photosynthetic activity and nutritional status of Trigonella foenum-graecum L. *Crop & Pasture Science* 73:969–80
8. Liu Z, Tian L, Chen M, Zhang L, Lu Q, et al. 2023. Hormesis responses of growth and photosynthetic characteristics in *Lonicera japonica* Thunb. to cadmium stress: whether electric field can improve or not? *Plants* 12:933
9. Zhou J, Song F, He Y, Zhang W, Liang X, et al. 2023. LncRNA evolution and DNA methylation variation participate in photosynthesis pathways of distinct lineages of *Populus*. *Forestry Research* 3:3
10. Song Y and Jin G. 2023. Do tree size and tree shade tolerance affect the photosynthetic capacity of broad-leaved tree species? *Plants* 12:523
11. Schmiege SC, Griffin KL, Boelman NT, Vierling LA, Bruner SG, et al. 2023. Vertical gradients in photosynthetic physiology diverge at the latitudinal range extremes of white spruce. *Plant, Cell & Environment* 46:45–63
12. Kosugi Y, Takanashi S, Yokoyama N, Kamakura M. 2012. Vertical variation in leaf gas exchange parameters for a Southeast Asian tropical rainforest in Peninsular Malaysia. *Journal of Plant Research* 125:735–48
13. Chen X, Sun J, Lyu M, Wang M, Hu D, et al. 2021. Prediction of photosynthetic light-response curves using traits of the leaf economics spectrum for 75 woody species: effects of leaf habit and sun–shade dichotomy. *American Journal of Botany* 108:423–31
14. Wyka TP, Oleksyn J, Żytkowiak R, Karolewski P, Jagodziński AM, et al. 2012. Responses of leaf structure and photosynthetic properties to intra-canopy light gradients: a common garden test with four broadleaf deciduous angiosperm and seven evergreen conifer tree species. *Oecologia* 170:11–24
15. Coble AP, Cavaleri MA. 2014. Light drives vertical gradients of leaf morphology in a sugar maple (*Acer saccharum*) forest. *Tree Physiology* 34:146–58
16. Coble AP, Vanderwall B, Mau A, Cavaleri MA. 2016. How vertical patterns in leaf traits shift seasonally and the implications for modeling canopy photosynthesis in a temperate deciduous forest. *Tree Physiology* 36:1077–91

17. Liu Q, Li F. 2018. Spatial and seasonal variations of standardized photosynthetic parameters under different environmental conditions for young planted *Larix olgensis* Henry trees. *Forests* 9:522
18. Martin RE, Asner GP, Bentley LP, Shenkin A, Salinas N, et al. 2019. Covariance of sun and shade leaf traits along a tropical forest elevation gradient. *Frontiers in Plant Science* 10:1810
19. Koch GW, Sillett SC, Jennings GM, Davis SD. 2004. The limits to tree height. *Nature* 428:851–54
20. Hata Y, Kumagai T, Shimizu T, Miyazawa Y. 2023. Implications of seasonal changes in photosynthetic traits and leaf area index for canopy CO_2 and H_2O fluxes in a Japanese cedar (*Cryptomeria japonica* D. Don) plantation. *Ecological Modelling* 477:110271
21. Collier DE, Thibodeau BA. 1995. Changes in respiration and chemical content during autumnal senescence of *Populus tremuloides* and *Quercus rubra* leaves. *Tree Physiology* 15:759–64
22. Wyka TP, Żytkowiak R, Oleksyn J. 2016. Seasonal dynamics of nitrogen level and gas exchange in different cohorts of Scots pine needles: a conflict between nitrogen mobilization and photosynthesis? *European Journal of Forest Research* 135:483–93
23. Yin H, Yang M, Li P, Yu X, Xiong H, et al. 2022. Seasonality of photosynthetic physiology and leaf anatomy in three different *Quercus* L. Section *Cyclobalanopsis* seedlings of *Quercus chungii*, *Quercus gilva*, and *Quercus glauca* in the subtropical region of South China. *Forests* 13:2067
24. Shimada R, Takahashi K. 2022. Diurnal and seasonal variations in photosynthetic rates of dwarf pine *Pinus pumila* at the treeline in central Japan. *Arctic, Antarctic, and Alpine Research* 54:1–12
25. Atkin OK, Bloomfield KJ, Reich PB, Tjoelker MG, Asner GP, et al. 2015. Global variability in leaf respiration in relation to climate and leaf traits. *New Phytologist* 206:614–36
26. Coble AP, Cavaleri MA. 2015. Light acclimation optimizes leaf functional traits despite height-related constraints in a canopy shading experiment. *Oecologia* 177:1131–43
27. Xu M, Wang Q, Yang F, Zhang T, Zhu X, et al. 2022. The responses of photosynthetic light response parameters to temperature among different seasons in a coniferous plantation of subtropical China. *Ecological Indicators* 145:109595
28. Zlobin IE, Kartashov AV, Pashkovskiy PP, Ivanov YV, Kreslavski VD, et al. 2019. Comparative photosynthetic responses of Norway spruce and Scots pine seedlings to prolonged water deficiency. *Journal of Photochemistry and Photobiology B: Biology* 201:111659
29. Coble AP, Cavaleri MA. 2017. Vertical leaf mass per area gradient of mature sugar maple reffects both height-driven increases in vascular tissue and light-driven increases in palisade layer thickness. *Tree Physiology* 37:1337–51
30. Xiong D, Flexas J. 2021. Leaf anatomical characteristics are less important than leaf chemical properties in determining photosynthesis responses to top-dress N. *Journal of Experimental Botany* 72:5709–20
31. Li W, Li J, Wei J, Niu C, Yang D, et al. 2023. Response of photosynthesis, the xanthophyll cycle, and wax in Japanese yew (*Taxus cuspidata* L.) seedlings and saplings under high light conditions. *PeerJ* 11:e14757
32. Mayoral C, Calama R, Sánchez-González M, Pardos M. 2015. Modelling the influence of light, water and temperature on photosynthesis in young trees of mixed Mediterranean forests. *New Forests* 46:485–506
33. Kitao M, Yazaki K, Tobita H, Agathokleous E, Kishimoto J, et al. 2022. Exposure to strong irradiance exacerbates photoinhibition and suppresses N resorption during leaf senescence in shade-grown seedlings of fullmoon maple (*Acer japonicum*). *Frontiers in Plant Science* 13:6413
34. Hazrati S, Tahmasebi-Sarvestani Z, Modarres-Sanavy SAM, Mokhtassi-Bidgoli A, Nicola S. 2016. Effects of water stress and light intensity on chlorophyll fluorescence parameters and pigments of *Aloe vera* L. *Plant Physiology and Biochemistry* 106:141–48
35. Xu H, Xiao J, Zhang Z, Ollinger SV, Hollinger DY, et al. 2020. Canopy photosynthetic capacity drives contrasting age dynamics of resource use efficiencies between mature temperate evergreen and deciduous forests. *Global Change Biology* 26:6156–67
36. He X, Si J, Zhou D, Wang C, Zhao C, et al. 2022. Leaf chlorophyll parameters and photosynthetic characteristic variations with stand age in a typical desert species (*Haloxylon ammodendron*). *Frontiers in Plant Science* 13:967849
37. Letts MG, Phelan CA, Johnson DRE, Rood SB. 2008. Seasonal photosynthetic gas exchange and leaf reflectance characteristics of male and female cottonwoods in a riparian woodland. *Tree Physiology* 28:1037–48
38. Liu Q, Xie L, Dong L, Li F. 2021. Dynamic simulation of the multilayer crown net photosynthetic rate and determination of the functional crown for larch (*Larix olgensis*) trees. *New Forests* 52:1011–35
39. Bassman JH, Zwier JC. 1991. Gas exchange characteristics of *Populus trichocarpa, Populus deltoides* and *Populus trichocarpa* × *P. deltoids clones*. *Tree Physiology* 8:145–59
40. R Core Team 2022. R: A language and environment for statistical computing. R Foundation for Statistical Computing, Vienna, Austria. Available online at https://www.R-project.org/.
41. Woodruff DR. 2014. The impacts of water stress on phloem transport in Douglas-fir trees. *Tree Physiology* 34:5–14
42. Zhang Y, Equiza MA, Zheng Q, Tyree MT. 2012. Factors controlling plasticity of leaf morphology in *Robinia pseudoacacia L.* II: the impact of water stress on leaf morphology of seedlings grown in a controlled environment chamber. *Annals of Forest Science* 69:39–47
43. Coble AP, Autio A, Cavaleri MA, Binkley D, Ryan MG. 2014. Converging patterns of vertical variability in leaf morphology and nitrogen across seven *Eucalyptus* plantations in Brazil and Hawaii, USA. *Trees-structure and Function* 28:1–15
44. Ambrose AR, Sillett SC, Dawson TE. 2009. Effects of tree height on branch hydraulics, leaf structure and gas exchange in California redwoods. *Plant, Cell & Environment* 32:743–57
45. Weerasinghe LK, Creek D, Crous KY, Xiang S, Liddell MJ, et al. 2014. Canopy position affects the relationships between leaf respiration and associated traits in a tropical rainforest in Far North Queensland. *Tree Physiology* 34:564–84
46. Mullin LP, Sillett SC, Koch GW, Tu KP, Antoine ME. 2009. Physiological consequences of height-related morphological variation in *Sequoia sempervirens* foliage. *Tree Physiology* 29:999–1010
47. Puglielli G, Varone L, Gratani L, Catoni R. 2017. Specific leaf area variations drive acclimation of *Cistus salvifolius* in different light environments. *Photosynthetica* 55:31–40
48. Oguchi R, Hikosaka K, Hirose T. 2005. Leaf anatomy as a constraint for photosynthetic acclimation: differential responses in leaf anatomy to increasing growth irradiance among three deciduous trees. *Plant, Cell & Environment* 28:916–27
49. Broeckx LS, Fichot R, Verlinden MS, Ceulemans R. 2014. Seasonal variations in photosynthesis, intrinsic water-use efficiency and stable isotope composition of poplar leaves in a short-rotation plantation. *Tree Physiology* 34:701–715
50. Riikonen J, Oksanen E, Peltonen P, Holopainen T, Vapaavuori E. 2003. Seasonal variation in physiological characteristics of two silver birch clones in the field. *Canadian Journal of Forest Research* 33:2164–76
51. Pieruschka R, Albrecht H, Muller O, Berry JA, Klimov D, et al. 2014. Daily and seasonal dynamics of remotely sensed photosynthetic efficiency in tree canopies. *Tree Physiology* 34:674–85
52. Misson L, Tu KP, Boniello RA, Goldstein AH. 2006. Seasonality of photosynthetic parameters in a multi-specific and vertically complex forest ecosystem in the Sierra Nevada of California. *Tree Physiology* 26:729–41
53. Grassi G, Vicinelli E, Ponti F, Cantoni L, Magnani F. 2005. Seasonal and interannual variability of photosynthetic capacity in relation

to leaf nitrogen in a deciduous forest plantation in northern Italy. *Tree Physiology* 25:349–60

54. Sperlich D, Chang CT, Peñuelas J, Gracia C, Sabaté S. 2015. Seasonal variability of foliar photosynthetic and morphological traits and drought impacts in a Mediterranean mixed forest. *Tree Physiology* 35:501–20
55. Pardos M, Puértolas J, Madrigal G, Garriga E, De Blas S, et al. 2010. Seasonal changes in the physiological activity of regeneration under a natural light gradient in a *Pinus pinea* regular stand. *Forest Systems* 19:367–80
56. Kunert N, Hajek P, Hietz P, Morris H, Rosner S, et al. 2022. Summer temperatures reach the thermal tolerance threshold of photosynthetic decline in temperate conifers. *Plant Biology* 24:1254–61
57. Yasumura Y, Hikosaka K, Hirose T. 2006. Seasonal changes in photosynthesis, nitrogen content and nitrogen partitioning in *Lindera umbellata* leaves grown in high or low irradiance. *Tree Physiology* 26:1315–23
58. Rodríguez-calcerrada J, Atkin OK, Robson TM, Zaragoza-castells J, Gil L, et al. 2010. Thermal acclimation of leaf dark respiration of beech seedlings experiencing summer drought in high and low light environments. *Tree Physiology* 30:214–24
59. Radoglou K, Teskey RO. 1997. Changes in rates of photosynthesis and respiration during needle development of loblolly pine. *Tree Physiology* 17:485–88
60. Vose JM, Ryan MG. 2002. Seasonal respiration of foliage, fine roots, and woody tissues in relation to growth, tissue N, and photosynthesis. *Global Change Biology* 8:182–93
61. Walters RG. 2005. Towards an understanding of photosynthetic acclimation. *Journal of Experiment Botany* 56:435–47
62. Way DA, Sage RF. 2008. Thermal acclimation of photosynthesis in black spruce [*Picea mariana* (Mill.) B.S.P.]. *Plant, Cell & Environment* 31:1250–62
63. Wieser G, Oberhuber W, Walder L, Spieler D, Gruber A. 2010. Photosynthetic temperature adaptation of *Pinus cembra* within the timberline ecotone of the Central Austrian Alps. *Annals of Forest Science* 67:201
64. Han Q, Kawasaki T, Katahata S, Mukai Y, Chiba Y. 2003. Horizontal and vertical variations in photosynthetic capacity in a *Pinus densiflora* crown in relation to leaf nitrogen allocation and acclimation to irradiance. *Tree Physiology* 23:851–57
65. Fellner H, Dirnberger GF, Sterba H. 2016. Specific leaf area of European Larch (*Larix decidua* MILL.). *Trees* 30:1237–44
66. Meinzer FC, Bond BJ, Karanian JA. 2008. Biophysical constraints on leaf expansion in a tall conifer. *Tree Physiology* 28:197–206
67. Han Q. 2011. Height-related decreases in mesophyll conductance, leaf photosynthesis and compensating adjustments associated with leaf nitrogen concentrations in *Pinus densiflora*. *Tree Physiology* 31:976–84
68. Marshall JD, Monserud RA. 2003. Foliage height influences specific leaf area of three conifer species. *Canadian Journal of Forest Research* 33:164–70